Chemical Engineering Journal 283 (2016) 1384–1391

Contents lists available at ScienceDirect

Chemical Engineering Journal

journal homepage: www.elsevier.com/locate/cej

Intrinsic kinetics of clofibric acid photocatalytic degradation in a fixed-film reactor

Agustina Manassero, Silvia Mercedes Zacarías, María Lucila Satuf, Orlando Mario Alfano *

Instituto de Desarrollo Tecnológico para la Industria Química (Universidad Nacional del Litoral and Consejo Nacional de Investigaciones Científicas y Técnicas), Güemes 3450, 3000 Santa Fe, Argentina

HIGHLIGHTS

- TiO_2 Aeroxide P25 is immobilized on the reactor glass window.
- Mass transfer limitations are analyzed.
- Kinetic modeling and experimental validation is presented.
- Radiation absorption by the catalytic film is calculated and included in the model.
- Intrinsic kinetic parameters are obtained.

GRAPHICAL ABSTRACT

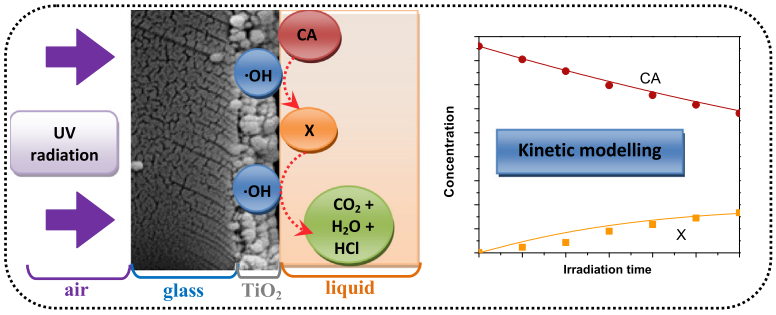

ARTICLE INFO

Article history:
Received 20 May 2015
Received in revised form 10 August 2015
Accepted 11 August 2015
Available online 28 August 2015

Keywords:
Photocatalysis
Intrinsic kinetics
Immobilized TiO_2
Clofibric acid

ABSTRACT

This study presents a kinetic model for the photocatalytic degradation of an organic pollutant in a fixed-film reactor for water treatment. The pharmaceutical drug clofibric acid (CA) was chosen as the model compound. Experiments were carried out employing TiO_2 Aeroxide P25 immobilized on the glass window of a laboratory scale reactor under UV radiation. A kinetic model to represent the degradation of CA was proposed, which explicitly takes into account the absorption of radiation by the catalytic film. Experimental results for different irradiation conditions and different number of TiO_2 coatings were used to estimate intrinsic kinetic parameters. External and internal mass transfer limitations were found to be negligible under our operating conditions. Good agreement was obtained between experimental data and model predictions, with a root mean square error of 9.9%.

1. Introduction

Heterogeneous photocatalysis with titanium dioxide (TiO_2) is an advance oxidation process that has been extensively studied to remove organic pollutants from water streams. One of the main advantages of photocatalysis is that it can mineralize organic molecules and/or transform initially biorecalcitrant compounds into biodegradable intermediates.

Up to now, most research on the application of heterogeneous photocatalysis for water treatment has been carried out in slurry reactors, where TiO_2 particles are suspended in aqueous solution. This configuration provides high surface area for adsorption and reaction but it requires the separation of the particles after reaction, which is undesirable from a practical and economic standpoint. This limitation can be overcome by immobilizing the catalyst over a suitable support, although mass transfer problems outside and/or inside the TiO_2 film are likely to occur [1–3].

Intrinsic kinetic parameters, useful for the design and optimization of photocatalytic devices, can be obtained from carefully

* Corresponding author. Tel.: +54 342 4511546; fax: +54 342 4511087.
E-mail address: alfano@santafe-conicet.gov.ar (O.M. Alfano).

http://dx.doi.org/10.1016/j.cej.2015.08.060
1385-8947/

Nomenclature

A_{cat}	catalytic area (cm^2)
C_i	bulk concentration of species i (i = CA, X) in terms of carbon content (mol cm^{-3})
D_e	effective diffusion coefficient (m^2 s^{-1})
$e_f^{a,s}$	surface rate of photon absorption by the TiO_2 film (nEinstein s^{-1} cm^{-2})
k	apparent kinetic constant (s^{-1})
H	thickness of the TiO_2 film (μm, m)
N	number of experimental data
$q_{f,in}$	local radiative flux that reaches the TiO_2 film (nEinstein s^{-1} cm^{-2})
$q_{f,tr}$	local radiative flux transmitted through the TiO_2 film (nEinstein s^{-1} cm^{-2})
$q_{f,rf}$	local radiative flux reflected by the TiO_2 film (nEinstein s^{-1} cm^{-2})
r	surface degradation rate (mol s^{-1} cm^{-2})
R	reflectance (dimensionless)
t	time (min, s)
T	transmittance (dimensionless)
V_T	total volume (mL)
X	organic intermediates

Acronyms

CA	clofibric acid
LSRPA	local surface rate of photon absorption (nEinstein s^{-1} cm^{-2})
RMSE	root mean square error
TOC	total organic carbon

Greek letters

α_f	fraction of energy absorbed by the TiO_2 films (dimensionless)
$\alpha_i (i = 1....5)$	intrinsic kinetic parameter
φ_λ	normalized fraction of radiation that reaches the coated window at wavelength λ (dimensionless)
Φ	Thiele modulus (dimensionless)

Subscripts

λ	relative to a specific wavelength
exp	experimental value
f	relative to a property of the TiO_2 film
fg	relative to a property of the TiO_2 film + glass
g	relative to a property of the bare borosilicate glass plate

Special symbol

⟨⟩	average

planned experiments and accurate models that take into account the influence of radiation, mass transfer and fluid dynamics on the reaction rate. When modeling reactors with immobilized catalyst, different approaches have been reported to incorporate the effect of radiation on reaction rate expressions. Nevertheless, most of them only consider the incident radiation at the catalyst surface [4,5] or assume monochromatic radiation although polychromatic radiation is used [6]. The most accurate approach involves the calculation of the radiation effectively absorbed by the photocatalytic film in the whole range of wavelengths employed.

The present work focuses on the development of a kinetic model to represent the degradation of an organic compound in a fixed-film photocatalytic reactor. The TiO_2 film was deposited over the flat, glass window of a cylindrical reactor, placed inside a batch recycling system and irradiated from one side by a UV lamp. Clofibric acid (CA) was chosen as the model pollutant. CA is the active metabolite of clofibrate, a pharmaceutical widely employed as blood lipid regulator. Due to its polar character, CA is poorly adsorbed in the subsoil and it can easily spread in surface water and groundwater. CA is also resistant to biodegradation and it has a very high persistence in the environment [7].

Experiments were carried out by varying the liquid flow rate, the irradiation intensity, and the TiO_2 film thickness. The influence of internal and external mass transfer on the reaction rate was also evaluated.

The rate of photon absorption by the TiO_2 film, which is explicitly included in the kinetic expressions, was computed from a radiation model and spectrophotometric measurements of TiO_2 coated plates. The mass of catalyst immobilized over the window and the thickness of the films were also assessed.

Finally, intrinsic kinetic parameters were calculated by fitting the model with experimental data. The model predicts the evolution of CA and its organic intermediates as a function of the irradiation time.

2. Materials and methods

2.1. Experimental setup

Photocatalytic experiments were carried out in a recirculating batch system consisting of a glass photoreactor, a peristaltic pump (Masterflex) and a storage tank with a sampling valve. The volume of the reactor was 54 mL and the total volume of the reacting solution in the system was 1000 mL (V_T). The isothermal condition (25 °C) was achieved by the incorporation of a water-circulating jacket to the storage tank. The reactor was cylindrical with two circular flat windows. It was illuminated through one of the windows, made of borosilicate ground glass, by a halogenated mercury lamp (150 W Powerstar HQI-TS from OSRAM). The lamp, with emission in the UV and visible range (350–780 nm), was placed at the focal axis of a parabolic reflector. In order to block the entrance of visible radiation to the reactor, a container with a solution of $CoSO_4$ was interposed between the reactor and the lamp. The wavelengths of the resulting radiation that arrives at the reactor window were comprised between 350 nm and 410 nm. Fig. 1 shows a schematic representation of the reactor and irradiation system. Optical neutral filters were used to carry out experiments at different irradiation levels: 100%, 62%, and 30%. These filters attenuate the incident radiation without altering the spectral distribution of the lamp. The incident radiation fluxes at the reactor window, experimentally measured by ferrioxalate actinometry [8], were 0.152 nEinstein s^{-1} cm^{-2}, 9.39 nEinstein s^{-1} cm^{-2}, and 4.58 nEinstein s^{-1} cm^{-2} for 100%, 62%, and 30%, respectively.

2.2. Catalyst immobilization

The catalyst (TiO_2 Aeroxide P25, Evonik Degussa GmbH, Germany) was immobilized over the inner face of the illuminated reactor window by the dip-coating technique. The surface of the window was grounded to improve the adherence of the catalyst to the glass. The dip coating is a technique widely employed to

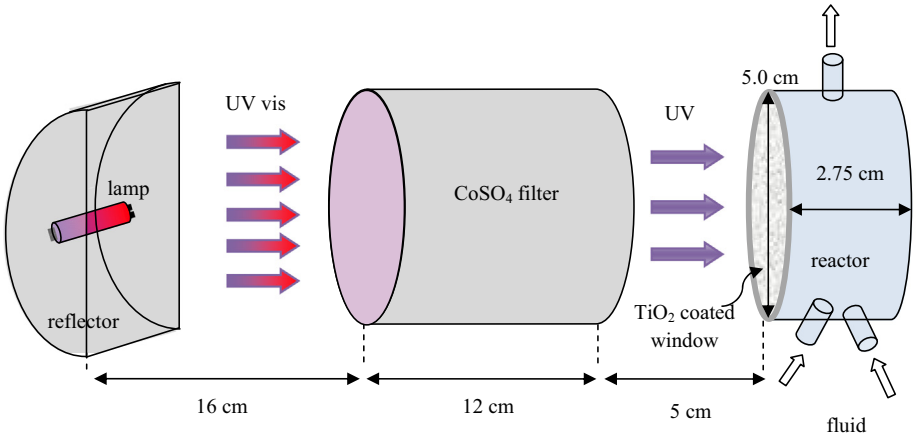

Fig. 1. Schematic representation of the reactor and irradiation system.

immobilize TiO_2 onto different supports [9]. This method basically consists of immersing the glass to be coated in a catalyst suspension and then withdrawing it at a controlled speed. Previous to the coating procedure, the window was washed with a solution containing 20 g of potassium hydroxide, 250 mL of isopropyl alcohol, and 250 mL of ultrapure water. The window remained in contact with the washing solution for 24 h and then for 2 h under sonication. Then, it was heated at 500 °C for 8 h to remove all traces of organic material.

A suspension of 150 g L^{-1} of TiO_2 in ultrapure water at pH 1.5, adjusted with HNO_3, was employed for the coatings [10]. The glass window was dipped into the TiO_2 suspension at room temperature (25 °C) and extracted at a constant withdrawal speed of 3 cm min^{-1}. Afterwards, the coated window was dried in an oven at 110 °C for 24 h and then calcined at 500 °C for 2 h at a heating rate of 5 °C min^{-1}. To increase the number of coatings over the window, the dipping/calcinations steps were repeated.

2.3. Characterization of the photocatalytic films

The thicknesses of the TiO_2 films were calculated from SEM images acquired by a Scanning Electron Microscope (JEOL, JSM-35C) equipped with an acquisition system of digital images (SemAfore).

The mass of TiO_2 immobilized per cm^2 of support was quantified by a spectrophotometric technique adapted from Jackson et al. [11], which involves the acidic digestion of the catalyst fixed on the glass support followed by the addition of H_2O_2 to form a colored complex, and a photometric detection at 410 nm. A detailed description of the procedure can be found in Zacarías et al. [12].

2.4. Photocatalytic experiments and sample analysis

To prepare the reacting solution, 20 mg of CA were placed in a volumetric flask. Ultrapure water was then added to dissolve the pollutant, and the resultant solution was diluted to a total volume of 1000 mL. The CA solution was added to the tank and circulated in the reactor for 60 min to achieve the adsorption equilibrium between CA and the TiO_2 film. During this time, the solution was saturated with pure oxygen by intense bubbling and the lamp was turned on to stabilize the radiation emission. To prevent the arrival of radiation at the reactor, a shutter was placed between the lamp and the reactor window. When the system was stabilized and the adsorption equilibrium was reached, the first sample was taken from the tank ($t = 0$) and then the shutter was removed. Throughout the reaction, the system was maintained under overpressure of oxygen to guarantee the renewal of the oxygen consumed. Each experiment lasted 480 min.

CA concentration was measured by HPLC with a UV detector using a Waters chromatograph provided with a RP C-18 column (XTerra®). The mobile phase was a binary mixture of acidified water (with 0.1% v/v phosphoric acid) and acetonitrile (50:50). Absorbance detection was made at 227 nm [13]. The organic content of the reacting solution was assessed by total organic carbon (TOC) analysis, employing a Shimadzu TOC-5000 A analyzer.

Experiments were carried out by varying the number of coatings on the reactor window, the incident radiation level and the flow rate. All experiments were performed at the same initial concentration of CA and the same initial pH. The operating conditions are summarized in Table 1. The effect of the solution pH on CA degradation was studied in previous experiments. A set of runs was carried out at pH 2, pH 5 (natural), and pH 10. The highest CA conversion was obtained at pH 5 and, therefore, natural pH was selected as the initial condition [14]. The evolution of pH was monitored throughout the experiments and no appreciable changes were observed.

Additional experiments (each one involving 6 h of reaction) were carried out to evaluate the possible loss of activity of the catalytic film, employing the window with 3 TiO_2 coatings. Loss of activity was not appreciable after four cycles of use of the catalytic window.

3. Kinetic model

The kinetic model proposed for the photocatalytic degradation of CA is based on a reaction scheme summarized in Table 2, which involves the attack of CA molecules by hydroxyl radicals, generating a single family of organic intermediates (X), which, in turn, can be mineralized by further radical oxidation. CA and X are assumed to compete with the same adsorption sites of the catalyst. This simplified approach considers that the mineralization of the original pollutant is accomplished through one "ideal" intermediate

Table 1
Operating conditions.

Parameter	Value
Initial concentration of CA (mol cm^{-3})	9.30×10^{-8}
pH	Natural (5)
Number of TiO_2 coatings	1–3–5
Irradiation level (%)	30–62–100
Flow rate (L min^{-1})	0.6–1.0–1.5–2.0

Table 2
Simplified reaction scheme for the photocatalytic degradation of CA.

Step	Reaction
Activation	$TiO_2 + h\nu \rightarrow e^- + h^+$
Recombination	$h^+ + e^- \rightarrow$ heat
Electron trapping	$e^- + O_{2,ads} \rightarrow \cdot O^-_{2,ads}$
Hole trapping	$h^+ + H_2O_{ads} \rightarrow \cdot OH + H^+$
Hydroxyl attack	$CA_{ads} + \cdot OH \rightarrow X$
	$X_{ads} + \cdot OH \rightarrow\rightarrow CO_2 + H_2O + HCl$

[5,15]. At any moment, the total organic carbon in the reacting solution is composed by the carbon due to CA and the carbon due to the presence of the reaction intermediates X. TOC concentration is calculated by TOC analysis and CA concentration is calculated by HPLC analysis. Therefore, the concentration of reaction intermediates X can be estimated by subtracting the concentration of carbon due to CA from the TOC concentration in solution.

The analytical expressions of the degradation rates of CA and X on the surface of the catalytic film, $r_{CA}(\mathbf{x}, t)$ and $r_X(\mathbf{x}, t)$, can be obtained following a similar procedure as the one detailed in our previous work [14]:

$$r_{CA}(\mathbf{x}, t) = \frac{\alpha_2 C_{CA}(t)}{1 + \alpha_3 C_{CA}(t) + \alpha_4 C_X(t)} \left(-1 + \sqrt{1 + \alpha_1 e^{a,s}_f(\mathbf{x})}\right) \quad (1)$$

$$r_X(\mathbf{x}, t) = \frac{\alpha_5 C_X(t)}{1 + \alpha_3 C_{CA}(t) + \alpha_4 C_X(t)} \left(-1 + \sqrt{1 + \alpha_1 e^{a,s}_f(\mathbf{x})}\right) \quad (2)$$

where α_i ($i = 1 \ldots 5$) represents the kinetic parameters involved in the photocatalytic degradation of CA, C_{CA} and C_X are the bulk concentrations of CA and X in terms of carbon content, respectively, t denotes irradiation time, $\mathbf{x}$ is the position vector, and $e^{a,s}_f$ is the local surface rate of photon absorption (LSRPA); that is, the amount of photons absorbed per unit time and per unit area of irradiated TiO_2-coated surface. The area of irradiated TiO_2-coated surface is the area of the support that is coated by the catalyst and is irradiated.

4. Results and discussion

4.1. Characterization of the photocatalytic films

Fig. 2 shows SEM images of the cross section of the glass window with 1, 3, and 5 coatings of TiO_2. In Table 3, the average thicknesses of the TiO_2 coatings and the amounts of TiO_2 immobilized on the glass supports, with the corresponding 95% confidence intervals, are reported.

4.2. Calculation of the absorbed radiation by the TiO_2 films

The spectral LSRPA in the TiO_2 film ($e^{a,s}_{f,\lambda}$) can be calculated by a radiation balance in terms of the local net radiation fluxes (Fig. 3):

$$e^{a,s}_{f,\lambda}(\mathbf{x}) = q_{f,\lambda,in}(\mathbf{x}) - q_{f,\lambda,tr}(\mathbf{x}) - q_{f,\lambda,rf}(\mathbf{x}) \quad (3)$$

where $q_{f,\lambda,in}(\mathbf{x})$ is the local radiative flux that reaches the TiO_2 film, $q_{f,\lambda,tr}(\mathbf{x})$ the local radiative flux transmitted through film, and $q_{f,\lambda,rf}(\mathbf{x})$ the local radiative flux reflected by the TiO_2 coating. Due to the design characteristics of the irradiation system and reactor, the coated window can be considered uniformly irradiated [14]. Therefore, averaged values of the radiation fluxes over the catalytic area (A_{cat}) may be used to obtain the rate of photon absorption:

$$\langle e^{a,s}_{f,\lambda} \rangle_{A_{cat}} = \langle q_{f,\lambda,in} \rangle_{A_{cat}} - \langle q_{f,\lambda,tr} \rangle_{A_{cat}} - \langle q_{f,\lambda,rf} \rangle_{A_{cat}} \quad (4)$$

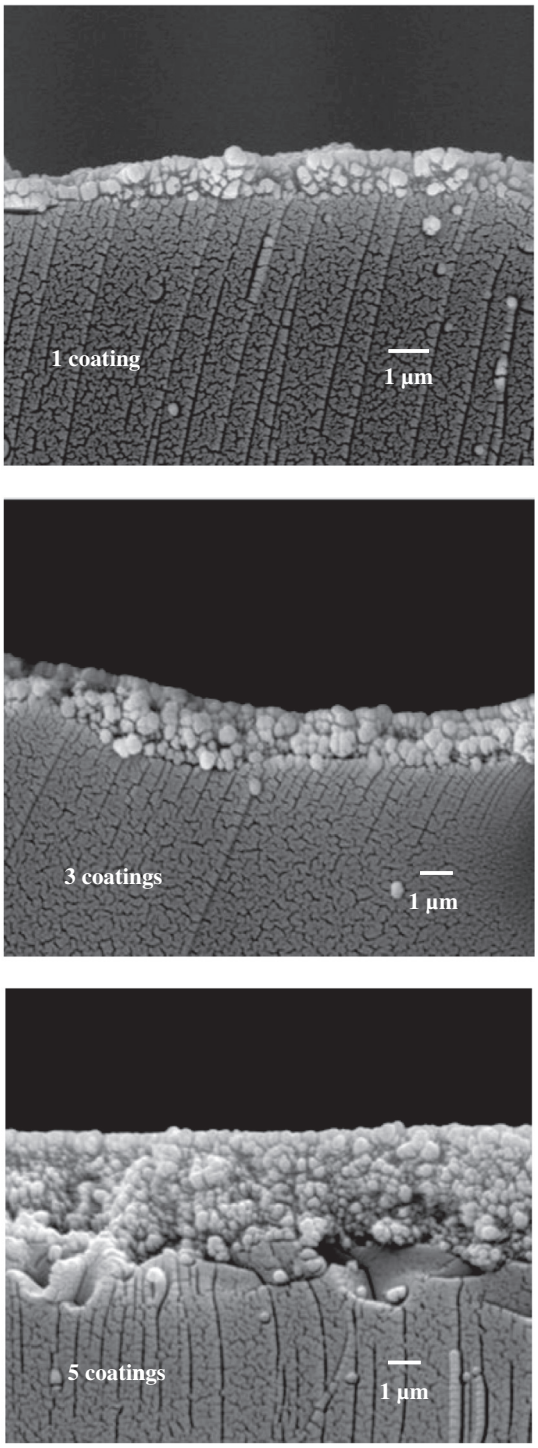

Fig. 2. Cross sectional SEM images of the TiO_2 film over glass plates.

Table 3
Film thickness and mass of catalyst immobilized over glass plates for different number of TiO_2 coatings.

Number of TiO_2 coatings	Film thickness (μm)	Mass of TiO_2 (mg cm^{-2})
1	0.65 ± 0.07	0.23 ± 0.01
3	1.70 ± 0.20	0.61 ± 0.01
5	2.70 ± 0.50	1.01 ± 0.02

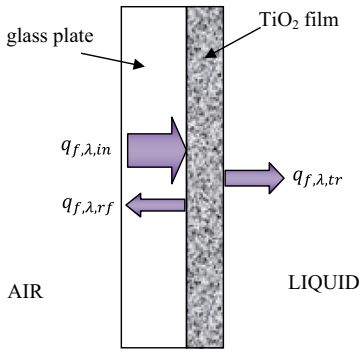

Fig. 3. Schematic representation of the radiation fluxes at the photocatalytic film.

The average surface rate of photon absorption can also be expressed as a function of the incident radiation flux as:

$$\langle e^{a,s}_{f,\lambda}\rangle_{A_{cat}} = \langle q_{f,\lambda,in}\rangle_{A_{cat}}\left(1-\frac{\langle q_{f,\lambda,tr}\rangle_{A_{cat}}}{\langle q_{f,\lambda,in}\rangle_{A_{cat}}}-\frac{\langle q_{f,\lambda,rf}\rangle_{A_{cat}}}{\langle q_{f,\lambda,in}\rangle_{A_{cat}}}\right) = \langle q_{f,\lambda,in}\rangle_{A_{cat}}\alpha_{f,\lambda} \quad (5)$$

where $\alpha_{f,\lambda}$ is the fraction of energy absorbed by the TiO_2 film at wavelength λ. Similarly, for polychromatic radiation:

$$\langle e^{a,s}_{f}\rangle_{A_{cat}} = \langle q_{f,in}\rangle_{A_{cat}}\sum_{\lambda}\alpha_{f,\lambda}\,\varphi_{\lambda} \quad (6)$$

In Eq. (6), φ_{λ} is the normalized fraction of radiation that reaches the coated plates at wavelength λ and $\sum_{\lambda}$ the summation over the useful wavelength range. φ_{λ} takes into account the spectral emission of the lamps (given by the manufacturer), the cut-off effect of the $CoSO_4$ filter and the slight modification of the lamp spectrum produced by the absorption of the borosilicate glass window. The average value of the incident radiation flux $\langle q_{f,in}\rangle_{A_{cat}}$ was experimentally measured by ferrioxalate actinometry, as stated in Section 2.1.

The absorbed fraction of energy $\alpha_{f,\lambda}$ can be calculated as:

$$\alpha_{f,\lambda} = 1 - T_{f,\lambda} - R_{f,\lambda} \quad (7)$$

where $T_{f,\lambda}$ and $R_{f,\lambda}$ represent the fraction of energy transmitted and reflected by the TiO_2 film at wavelength λ, respectively. $T_{f,\lambda}$ and $R_{f,\lambda}$ cannot be directly measured, but they can be computed from the experimental values of diffuse transmittance (T) and reflectance (R) of the coated and bare glass windows. The following expressions, obtained by applying the Net-Radiation method [16] to the coated plates, relate the values of transmittance and reflectance of the TiO_2 film (f), the bare glass plate (glass, g), and the coated glass plate (film + glass, fg):

$$R_{f,\lambda} = \frac{R_{fg,\lambda}T^2_{g,\lambda} - T^2_{fg,\lambda}R_{g,\lambda}}{T^2_{g,\lambda} - T^2_{fg,\lambda}R^2_{g,\lambda}} \quad (8)$$

$$T_{f,\lambda} = \frac{T_{fg,\lambda}}{T_{g,\lambda}}(1 - R_{f,\lambda}R_{g,\lambda}) \quad (9)$$

Diffuse transmittance and reflectance measurements of the coated and bare plates were carried out with a spectrophotometer Optronic OL series 750, equipped with a reflectance integrating sphere (OL 740-70). A detailed description of the methodology employed can be found in Zacarías et al. [12]. Fig. 4 shows data acquired for the glass window with 1, 3 and 5 TiO_2 coatings and for the bare glass.

Results of $\langle e^{a,s}_{f}\rangle_{A_{cat}}$ for the different irradiation conditions and number of coatings calculated with Eqs. (6)–(9), are presented in Table 4.

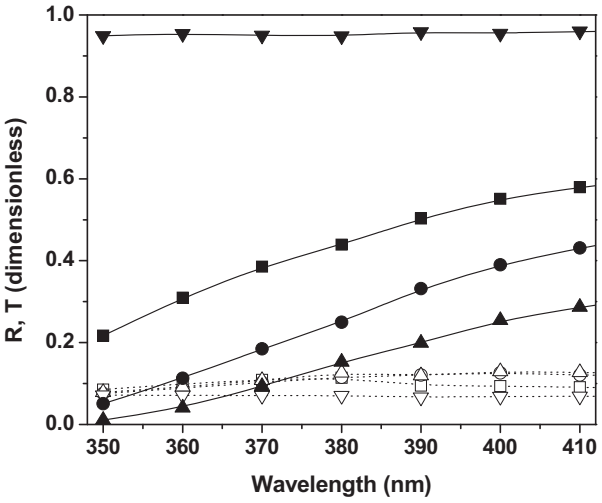

Fig. 4. Diffuse transmittance and reflectance of the coated and uncoated glass window as a function of wavelength. Open symbols: diffuse reflectance; filled symbols: diffuse transmittance. (□): 1 coating, (○): 3 coatings, (△): 5 coatings, (▽): uncoated glass.

Table 4
Absorbed radiation by the TiO_2 films under different experimental conditions.

Number of TiO_2 coatings	Irradiation level (%)	$\langle e^{a,s}_{f}\rangle_{A_{cat}}$ (nEinstein cm^{-2} s^{-1})
1	100	2.89
3	100	3.94
5	100	4.79
3	30	1.19
3	62	2.43

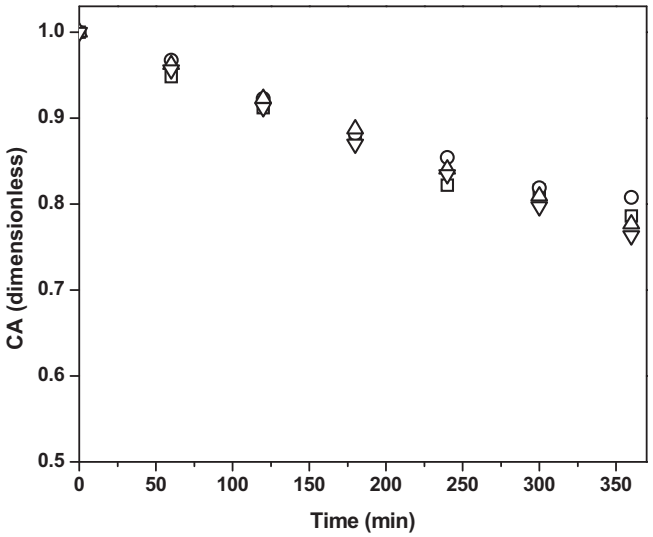

Fig. 5. CA concentration vs. time for different flow rates. □ 0.6 L min^{-1}; ○ 1.0 L min^{-1}, △ 1.5 L min^{-1} and ▽ 2.0 L min^{-1}.

4.3. Mass transfer limitations

When modeling photocatalytic reactors, especially in the case of supported catalyst, mass transfer phenomena have to be considered both outside (external mass transfer) and inside the film (internal mass transfer). External mass transfer limitations become

Table 5
Estimated kinetic parameters.

	Parameter	Value ± 95% CI	Units
5-Parameters model	α_1	(9.24 ± 0.18)	$cm^2\ s\ nEinstein^{-1}$
	α_2	$(1.51 \pm 0.48) \times 10^{-4}$	$cm\ s^{-1}$
	α_3	$(1.31 \pm 0.68) \times 10^{-2}$	$cm^3\ mol^{-1}$
	α_4	$(1.17 \pm 0.52) \times 10^{-2}$	$cm^3\ mol^{-1}$
	α_5	$(2.26 \pm 0.41) \times 10^{-4}$	$cm\ s^{-1}$
	RMSE%	9.8	
2-Parameters model	α'_2	$(4.58 \pm 1.1) \times 10^{-4}$	$cm^2\ s^{-1/2}\ nEinstein^{-1/2}$
	α'_5	$(6.86 \pm 1.5) \times 10^{-4}$	$cm^2\ s^{-1/2}\ nEinstein^{-1/2}$
	RMSE%	9.9	

important mainly when working at low flow rates, whereas internal mass transfer problems may arise when the thickness of the photocatalytic film is considerable. Both kinds of limitations have a direct effect on the reaction rate. Therefore, the modeling of a photocatalytic reactor needs a preliminary step to evaluate these phenomena.

To determine whether the reaction was limited by external mass transfer, a set of experimental runs were carried out at different flow rates employing the window with 3 TiO_2 coatings and 100% of irradiation level. The flow rate was increased from 0.6 L min^{-1} to 2.0 L min^{-1}.

As shown in Fig. 5, the rate of degradation of CA does not vary significantly with the flow rate. After 360 min of irradiation, the CA concentrations obtained at 1.5 L min^{-1} and 2.0 L min^{-1} differ by less than 1.8%, thus indicating that external mass transfer limitations are negligible under these experimental conditions. The flow rate employed in the kinetic experiments was 1.5 L min^{-1}.

On the other hand, the influence of internal mass transfer was estimated by the Thiele modulus (Φ) [17]:

$$\Phi = H\sqrt{\frac{k}{D_e}} \tag{10}$$

where H is the thickness of the film, k an apparent first order kinetic rate constant and D_e the effective diffusion coefficient. A small value of the Thiele modulus indicates that internal mass transfer resistance is negligible. Considering the information reported in the literature of D_e for organic compounds in a porous TiO_2 film, a value of $1.0 \times 10^{-10}\ m^2\ s^{-1}$ was adopted [2,18]. k was obtained from experimental data and H was determined from SEM images (Fig. 2).

The value computed for Φ in the most unfavorable situation (window with 5 coatings and 100% of irradiation level) is 0.001. This low value of Φ ($\Phi \ll 1$) allows assuming that the assumption that the internal mass transfer resistance is negligible.

4.4. Kinetic parameters estimation

Taking into account the considerations made in the previous section, the mass balances for CA and X in the reacting system with their respective initial conditions take the following form [19]:

$$\frac{dC_{CA}}{dt} = -\frac{A_{cat}}{V_T}\langle r_{CA}\rangle_{A_{cat}} = -\frac{A_{cat}}{V_T}\frac{\alpha_2 C_{CA}}{(1+\alpha_3 C_{CA}+\alpha_4 C_X)}\left\langle\left(-1+\sqrt{1+\alpha_1 e_f^{a,s}}\right)\right\rangle_{A_{cat}} \tag{11}$$

$$C_{CA}(t=0) = C_{CA,0}$$

$$\frac{dC_X}{dt} = \frac{A_{cat}}{V_T}\left[\langle r_{CA}\rangle_{A_{cat}} - \langle r_X\rangle_{A_{cat}}\right] = \frac{A_{cat}}{V_T}\frac{\alpha_2 C_{CA}-\alpha_5 C_X}{(1+\alpha_3 C_{CA}+\alpha_4 C_X)}\left\langle\left(-1+\sqrt{1+\alpha_1 e_f^{a,s}}\right)\right\rangle_{A_{cat}} \tag{12}$$

$$C_X(t=0) = 0$$

where $\langle r_i\rangle_{A_{cat}}$ (i = CA, X) represents the surface degradation rate of the organic compound averaged over the catalytic area (A_{cat} = 19.6 - cm^2). Eqs. (11) and (12) are valid in a well-mixed system considering that direct photolysis is neglected and chemical reactions take place at the solid–liquid interface.

The five kinetic parameters involved in Eqs. (11) and (12) were determined by fitting the model to the experimental data using the Levenberg–Marquardt optimization method [20].

From the analysis of the parameters estimation values, it was possible to neglect the terms $\alpha_3 C_{CA}$ and $\alpha_4 C_X$ in the denominator of Eqs. (11) and (12) due to the fact that they were much lower than 1. This means that, at the employed concentrations of CA and X, there is an excess of catalytic adsorption sites in the film and, therefore, the adsorption of one compound is not limited by the adsorption of the other. Additionally, the term $\alpha_1 e_f^{a,s}$ was much higher than 1 for all irradiation conditions. As a result, the term in parentheses in the mass balances can be simplified to $\sqrt{e_f^{a,s}}$ and the equations take the following form:

$$\frac{dC_{C_{CA}}}{dt} = -\frac{A_{cat}}{V_T}\alpha'_2 C_{CA}\left\langle\sqrt{e_f^{a,s}}\right\rangle_{A_{cat}} \tag{13}$$

$$\frac{dC_X}{dt} = \frac{A_{cat}}{V_T}\left(\alpha'_2 C_{CA}-\alpha'_5 C_X\right)\left\langle\sqrt{e_f^{a,s}}\right\rangle_{A_{cat}} \tag{14}$$

where $\alpha'_2 = \alpha_2\sqrt{\alpha_1}$ and $\alpha'_5 = \alpha_5\sqrt{\alpha_1}$.

The percentage root mean square error (RMSE%) of the model estimations was calculated according to Eq. (15).

$$\text{RMSE}\% = \sqrt{\frac{1}{N}\sum_{i=1}^{N}\left(\frac{C_{exp,i}-C_i}{C_{exp,i}}\right)^2}\times 100 \tag{15}$$

where N is the total number of concentrations evaluated (N = 80), $C_{exp,i}$ the concentration experimentally measured for CA and X, and C_i the corresponding concentration value predicted by the model.

The values of the estimated kinetic parameters for the generalized (5-parameters) and simplified (2-parameters) models, with the corresponding 95% confidence intervals and the RMSE%, are presented in Table 5.

It is important to note that the reduction from 5 to 2 parameters does not substantially increase the error of the estimations. Consequently, the 2-parameter kinetic model has been chosen to represent the model results. Fig. 6 depicts the experimental data and model predictions with the 2-parameters model for different experimental conditions.

These results show that the proposed kinetic model can adequately predict the evolution of the concentration of CA and of the organic intermediates formed in the degradation process under different conditions of irradiation and film thicknesses.

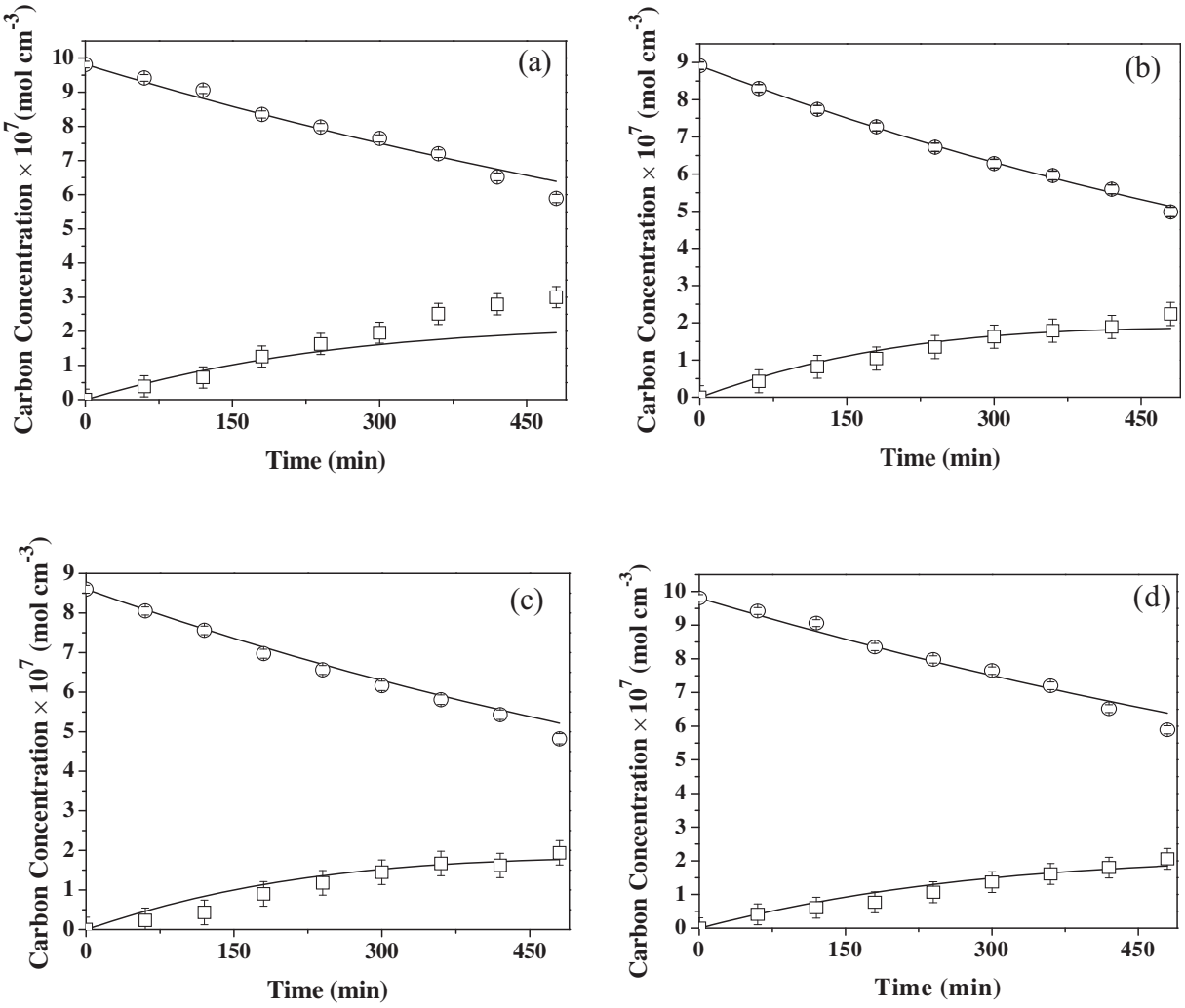

Fig. 6. Experimental and predicted concentrations of CA and X vs. irradiation time for different experimental conditions. Experimental data: ○: CA; □: X. Model results: solid lines. (a) 1 coating and 100% of irradiation level; (b) 3 coatings and 100% irradiation level; (c) 5 coatings and 100% irradiation level; (d) 3 coatings and 62% irradiation level.

5. Conclusions

An intrinsic kinetic model was proposed and validated to represent the clofibric acid photocatalytic degradation in a fixed-film reactor. This model was able to reproduce all the experimental data with only two kinetic parameters. Reliable kinetic information is essential to design efficient devices for water detoxification, which should tend to achieve maximum interaction between radiation, catalytic surface and pollutant molecules. In this study, the absorption of radiation by the TiO_2 film was modeled and evaluated; this information was explicitly included in the kinetic model expressions. Therefore, the obtained kinetic parameters are independent of the irradiation conditions or thicknesses of the films (within the limits of the experimental conditions tested) and can be applied to design, scaling-up, or optimize fixed-film photocatalytic reactors of different configurations.

Acknowledgements

The authors are grateful to Universidad Nacional del Litoral (UNL), Consejo Nacional de Investigaciones Científicas y Técnicas (CONICET), and Agencia Nacional de Promoción Científica y Tecnológica (ANPCyT) for financial support. We also thank Antonio C. Negro for his valuable help during the experimental work.

References

[1] M.F.J. Dijkstra, A. Michorius, H. Buwalda, H.J. Panneman, J.G.M. Winkelman, A. A.C.M. Beenackers, Comparison of the efficiency of immobilized and suspended systems in photocatalytic degradation, Catal. Today 66 (2001) 487–494.
[2] D. Chen, F. Li, A.K. Ray, External and internal mass transfer effect on photocatalytic degradation, Catal. Today 66 (2001) 475–485.
[3] G. Camera-Roda, F. Santarelli, Optimization of the thickness of a photocatalytic film on the basis of the effectiveness factor, Catal. Today 129 (2007) 161–168.
[4] D. Li, K. Xiong, W. Li, Z. Yang, C. Liu, X. Feng, X. Lu, Comparative study in liquid-phase heterogeneous photocatalysis: model for photoreactor scale-up, Ind. Eng. Chem. Res. 49 (2010) 8397–8405.
[5] M. Vezzoli, W.N. Martens, J.M. Bell, Investigation of phenol degradation: true reaction kinetics on fixed film titanium dioxide photocatalyst, Appl. Catal. A: General 404 (2011) 155–163.
[6] M. Vezzoli, T. Farrell, A. Baker, S. Psaltis, W.N. Martens, J.M. Bell, Optimal catalyst thickness in titanium dioxide fixed film reactors: mathematical modeling and experimental validation, Chem. Eng. J. 234 (2013) 57–65.
[7] R. Salgado, A. Oehmen, G. Carvalho, J.P. Noronha, M.A. Reis, Biodegradation of clofibric acid and identification of its metabolites, J. Hazard. Mater. 241–242 (2012) 182–189.
[8] S.L. Murov, I. Carmichael, G.L. Hug, Handbook of Photochemistry, second ed., Marcel Dekker, New York, 1993.
[9] A.Y. Shan, T.I.M. Ghazi, S.A. Rashid, Immobilization of titanium dioxide onto supporting materials in heterogeneous photocatalysis: a review, Appl. Catal. A: General 389 (2010) 1–8.
[10] R. Van Grieken, J. Marugán, C. Sordo, C. Pablos, Comparison of the photocatalytic disinfection of *E. coli* suspensions in slurry, wall and fixed-bed reactors, Catal. Today 144 (2009) 48–54.

[11] N.B. Jackson, C.M. Wang, Z. Luo, J. Schwitzgebel, J.G. Ekerdt, J.R. Brock, A. Heller, Attachment of TiO_2 powders to hollow glass microbeads. Activity of the TiO_2-coated beads in the photoassisted oxidation of ethanol to acetaldehyde, J. Electrochem. Soc. 138 (1991) 3660–3664.
[12] S.M. Zacarías, M.L. Satuf, M.C. Vaccari, O.M. Alfano, Efficiency evaluation of different TiO_2 coatings on the photocatalytic inactivation of airborne bacterial spores, Ind. Eng. Chem. Res. 51 (2012) 13599–13608.
[13] A. Dordio, A. Estêvão Candeias, A. Pinto, C. Teixeira da Costa, A. Palace Carvalho, Preliminary media screening for application in the removal of clofibric acid, carbamazepine and ibuprofen by SSF-constructed wetlands, Ecol. Eng. 35 (2009) 290–302.
[14] A. Manassero, M.L. Satuf, O.M. Alfano, Kinetic modeling of the photocatalytic degradation of clofibric acid in a slurry reactor, Environ. Sci. Pollut. Res. 22 (2015) 926–937.
[15] I.R. Bellobono, M. Rossi, A. Testino, F. Morazzoni, R. Bianchi, G. de Martini, P.M. Tozzi, R. Stanescu, C. Costache, L. Bobirica, M.L. Bonardi, F. Groppi, Influence of irradiance, flow rate, reactor geometry, and photopromoter concentration in mineralization kinetics of methane in air and in aqueous solutions by photocatalytic membranes immobilizing titanium dioxide, Int. J. Photoenergy 2008 (2008) 1–14.
[16] R. Siegel, J. Howell, Thermal Radiation Heat Transfer, fourth ed., Taylor and Francis, New York, 2002.
[17] G.F. Froment, J. DeWilde, K.B. Bischoff, Chemical Reactor Analysis and Design, third ed., Wiley, New York, 2011.
[18] S.M. Ould-Mame, O. Zahraa, M. Bouchy, Photocatalytic degradation of salicylic acid on fixed TiO_2 – kinetic studies, Int. J. Photoenergy 2 (2000) 59–66.
[19] J. Marugán, R. van Grieken, C. Pablos, M.L. Satuf, A.E. Cassano, O.M. Alfano, Kinetic modelling of *Escherichia coli* inactivation in a photocatalytic wall reactor, Catal. Today 240 (2015) 9–15.
[20] D.M. Himmelblau, Process Analysis by Statistical Methods, Wiley, New York, 1970.